Proceedings of the 2016 Winter Simulation Conference
T. M. K. Roeder, P. I. Frazier, R. Szechtman, E. Zhou, T. Huschka, and S. E. Chick, eds.

QUANTIFYING THE IMPACT OF MICROGRID LOCATION AND BEHAVIOR ON TRANSMISSION NETWORK CONGESTION

Jialin Liu

Department of Electrical and Computer Engineering
Cornell University
Ithaca, NY 14853, USA

Gabriela Martinez

Health Care Systems Engineering
Mayo Clinic
200 First ST. SW
Rochester, MN 55905, USA

C. Lindsay Anderson

Department of Biological and Environmental Engineering
Cornell University
Ithaca, NY 14853, USA

ABSTRACT

This work presents a preliminary analysis considering impact of a grid-connected microgrid on network transmission of the power system. The locational marginal prices of the power system are used to strategically place the microgrid to avoid congestion problems. In addition, a Monte Carlo simulation approach is implemented to confirm that network congestion can be attenuated if appropriate price-based signals are set to define the import and export dynamic between the two systems.

1 INTRODUCTION

Electricity generation accounts for nearly half of the total CO_2 emissions in the United States (EPA 2016). For this reason, the development and integration of renewable resources will play an essential role in achieving the societal objective of mitigating climate change through greenhouse gas emission reduction. In a clean and robust future grid, it is envisioned that distribution systems, which are currently strictly consumers, will become *microgrid* structures that are capable of both producing and consuming electricity. These systems will also have the capability to be self-sufficient through generation and storage of electricity, as well as the leveraging of flexible consumers. In times of excess generation, the microgrid could participate in wholesale electricity markets through provision of energy to the larger transmission system. To this end, the interaction between the microgrid and the transmission system is of significant interest. In particular, this paper considers the interaction between the transmission system and a simulated microgrid, and its potential role in congestion management.

There has been extensive research in the use of distributed generation (DG) for congestion management. For example, Afkousi-Paqaleh, Abbaspour-Tehrani-fard, Rashidinejad, and Lee (2010) considers optimal location of the DG by evaluating a number of candidate locations for a large number of possible loading scenarios, and selection of the location with the best cost/benefit ratio. Liu, Salama, and Mansour (2005) explore potential places for DG placement by calculating the contribution factors of DGs and creating a partition according to the index of the total amount of distributed resources available. A particle swarm optimization method is proposed to solve for the optimal location of DGs in Nabavi, Hajforoosh, and

Masoum (2011). A dynamic graph method is applied to identify the optimal buses to connect DGs in Labrini, Gad, ElShatshat, and Salama (2015). The work of Kumar, Dutta, and Xie (2011), Afkousi-Paqaleh, Noory, F., and Rashidinejad (2010) uses the idea of locational marginal price ranking to shrink the search space and find the optimal DG placement. A simulated annealing method is adopted for DG placement with regards to congestion management, in Nayanatara, Baskaran, and Kothari (2015).

In addition, power generated from renewable technologies, such as wind turbines or Photovoltaic (PV) solar panels, experiences sudden variations due to weather conditions. The intermittent nature of these renewable resources could create periods of high-volume power injection into the system, which may then cause system congestion. The work of Chun-Hao and Nirwan (2012) addresses congestion in the distribution network caused by surplus DG in the form of household rooftop PV panels. The congestion problem is solved by disconnecting certain PV panels in order to match supply and demand of the distribution network. In contrast, the congestion problem considered in our work is at the transmission system level, possibly caused by power transactions between the main utility and grid-connected systems, for example, microgrids. We tackle the congestion problem by setting import/export transaction pricing schemes to induce a desired transaction dynamic between the main utility and a grid-connected system.

Grid-connected microgrids are an important consideration in transmission congestion management, of particular interest due to their capability to consume and provide power through independent management of generation, storage and responsive demand. The flexibility of these structures could have a significant role in transmission line congestion alleviation, though the research in this area is minimal. Therefore, this study specifically considers transmission congestion management through the interaction of the main network and the microgrid, with a comprehensive model for each. The paper is organized as follows; in Section 2, the modeling framework is described for the transmission system, the microgrid, and the interaction between them. In Section 3, the specifics of the case study, and the numerical results, are described, while Section 4 provides discussion and conclusions.

2 MODEL

This work analyzes the interaction between the power grid and a microgrid located at a certain node of the transmission network. To this end, optimal power management of the microgrid and main grid (power system) are formulated within a time horizon, $\mathscr{T} := \{1,\dots,T\}$, of length T. The sections below introduce the optimization models used to determine the operation of the microgrid and the power grid.

2.1 Microgrid Power Management

The model presented in this section is based on the models proposed in (Zhang, Gatsis, and Giannakis 2013; Martinez, Gatsis, and Giannakis 2013). The microgrid considered is composed of small-scale conventional generators, renewable units, non-dispatchable and dispatchable loads, and a storage unit. More specifically, let M, J and N be the total number of conventional generators, renewable units, and dispatchable loads, respectively.

The power produced by a conventional generator is denoted by $P^t_{g_m}$, where $m \in \mathscr{M} := \{1,\dots,M\}$, the power production of a renewable unit is denoted by $P^t_{v_j}$, $j \in \mathscr{J} := \{1,\dots,J\}$, the power consumed by a dispatchable load is represented by $P^t_{d_n}$, $n \in \mathscr{N} := \{1,\dots,N\}$, and D^t is the non-dispatchable load at time period t. Let P^t_b be the power delivered to the storage unit, and b^t be the state of charge (SoC) of the storage unit at time period t. The following vector notations are used throughout the paper:

$$\mathbf{b} = [b^1,\dots,b^T], \quad \mathbf{p}_b = [P^1_b,\dots,P^T_b], \quad \mathbf{i}_p = [I^1_p,\dots,I^T_p], \quad \mathbf{e}_p = [E^1_p,\dots,E^T_p], \quad \mathbf{p}^t_g = [P^t_{g_1},\dots,P^t_{g_M}],$$
$$\mathbf{p}_g = [\mathbf{p}^1_g,\dots,\mathbf{p}^T_g], \quad \mathbf{p}^t_d = [P^t_{d_1},\dots,P^t_{d_N}], \quad \mathbf{p}_d = [\mathbf{p}^1_d,\dots,\mathbf{p}^T_d], \quad \mathbf{p}^t_v = [P^t_{v_1},\dots,P^t_{v_J}], \quad \mathbf{p}_v = [\mathbf{p}^1_v,\dots,\mathbf{p}^T_v],$$

The microgrid can purchase or sell power to the main grid at each period of time. The import (purchase) transaction cost is determined by a time-dependent non-negative piecewise linear convex function $\kappa^t_\iota(\cdot)$; exports (sells) are governed by a time-dependent non-negative piecewise linear concave function $\kappa^t_e(\cdot)$. It

is assumed that $\kappa_l^t(p) \geq \kappa_e^t(p)$ for all $p \geq 0$ and for all $t \in \mathscr{T}$ because the transaction rules are driven by the main grid.

Given the transaction costs and renewable power output over the time horizon, the total operational cost of the microgrid can be expressed as follows:

$$G(\mathbf{p}_d, \mathbf{p}_g, \mathbf{i}_p, \mathbf{e}_p, \mathbf{p}_b, \mathbf{b}) \;:=\; \sum_{t\in\mathscr{T}} \Big(\sum_{m\in\mathscr{M}} g_m(P_{g_m}^t) - \sum_{n\in\mathscr{N}} g_n(P_{d_n}^t) \Big) + \sum_{t\in\mathscr{T}} \big(g_b(b^t) + \kappa_l^t(I_p^t) - \kappa_e^t(E_p^t) \big),$$

where $g_m(\cdot)$ is the generation cost function of conventional generation, which is assumed to be convex, the concave function $g_n(\cdot)$ is the reward for serving a dispatchable load, and the linear function $g_b(\cdot)$ models the utilization cost of the storage unit. The variables I_p^t and E_p^t represent the import and export transactions at time period t, respectively.

The transactions with the main grid are determined in order to balance supply and demand of the microgrid:

$$\mathbf{1}^\top \mathbf{p}_g^t + \mathbf{1}^\top \mathbf{p}_v^t - \mathbf{1}^\top \mathbf{p}_d^t - P_b^t - D^t = E_p^t - I_p^t, \quad E_p^t \geq 0, I_p^t \geq 0 \quad , t \in \mathscr{T}, \tag{1}$$

where $\mathbf{1}$ is a vector whose coordinates are equal to one. Clearly, import transactions are caused when the microgrid is not able to meet the demand of its users, and any surplus of generated power could be exported to the main grid.

The operation of the conventional units is subject to the classical constraints included in any economic dispatch model (Martinez, Zhang, and Giannakis 2014):

$$\underline{P}_m \leq P_{g_m}^t \leq \bar{P}_m, \quad -R_m^d \leq P_{g_m}^t - P_{g_m}^{t-1} \leq R_m^u, \quad m \in \mathscr{M}, t \in \mathscr{T}, \tag{2}$$

where the generating bounds of each unit are denoted by $\underline{P}_m, \bar{P}_m$, and the ramping limits are R_m^d, R_m^u.

The dispatchable loads are satisfied within user-defined bounds $\underline{P}_n, \bar{P}_n$:

$$\underline{P}_n \leq P_{d_n}^t \leq \bar{P}_n, n \in \mathscr{N}, t \in \mathscr{T}. \tag{3}$$

The charging and discharging efficiency parameters of the storage unit are assumed to be ideal; non-ideal efficiency coefficients can be easily included by adding extra variables in the model, the reader is referred to (Mohsenian-Rad 2015) for a discussion about this topic. The amount of energy delivered to the storage unit is limited by $P^+ > 0$; similarly, the amount of energy taken is bounded by $P^- > 0$. Let b^0 be the initial SoC of the unit and denote its maximum capacity as $\bar{b}$; then, the SoC dynamic can be formulated with the following linear constraints:

$$b^t = b^{t-1} + P_b^t, \quad -P^- \leq P_b^t \leq P^+, \quad 0 \leq b^t \leq \bar{b}, \quad t \in \mathscr{T}. \tag{4}$$

The goal of the microgrid operator is to efficiently manage its resources, satisfy the power needs of its electricity-end users, and maximize its revenue. To this end, the dispatchable loads and the storage unit will be used as control mechanisms to reduce the potential purchases of energy caused by sudden variations of the power produced by the renewable resources. The optimal management of the microgrid is formulated as an economic dispatch problem:

$$\min_{\mathbf{p}_d, \mathbf{p}_g, \mathbf{i}_p, \mathbf{e}_p, \mathbf{p}_b, \mathbf{b}} G(\mathbf{p}_d, \mathbf{p}_g, \mathbf{i}_p, \mathbf{e}_p, \mathbf{p}_b, \mathbf{b}) \tag{5}$$

$$\text{subject to:} (1), (2), (3), (4). \tag{6}$$

It is important to remark that the piecewise linear convex (concave) structure of the transaction costs together with the assumption $\kappa_e^t(p) \leq \kappa_l^t(p)$ for all $p \geq 0$ guarantees convexity of the objective function (Bertsekas 1999), therefore the optimization problem listed above is a convex problem for every realization of the uncertain renewable generation $\mathbf{p}_v$.

2.2 Power System Day-ahead Unit Commitment

The unit commitment model (UC) of the main network follows classic formulations (Tahanan, van Ackooij, Frangioni, and Lacalandra 2015; Wu and Shahidehpour 2010; Liu, Martinez, Li, Mathieu, and Anderson 2016). The goal of the UC problem is to find a cost-effective set of units necessary to cover the demand that satisfies the operational rules of the units as well as the transmission constraints of the network. For $i \in \mathscr{I} := \{1,\dots,I\}$, let w_i^t and z_i^t be binary variables representing the status (on or off) and start-up of the i-th unit of the system, respectively. At each period of time t, the power reserve level of each unit is denoted as R_i^t and its generation output is P_i^t. As in the previous section bold lowercase letters are used to represent vectors; the generation cost of the power system is defined as:

$$F(\mathbf{w},\mathbf{z},\mathbf{p}) = \sum_{i\in\mathscr{I}}\sum_{t\in\mathscr{T}}(f_i w_i^t + s_i z_i^t + C_i(P_i^t)),$$

where for each unit $i \in \mathscr{I}$ the parameter f_i is the fixed generation cost, s_i is the start-up cost, and each $C_i(\cdot)$ is the generation cost function, which is assumed to be convex.

The transmission network is represented with a set of nodes (or buses) $\mathscr{K}$ and a set of lines (or branches) $\mathscr{L}$, the load forecast of the systems at each node is denoted as L_k^t, $k \in \mathscr{K}, t \in \mathscr{T}$. The power flow of the system is determined by the following constraints:

$$\theta = B^{-1}\mathbf{p}_k^t, \quad \mathbf{p}_\ell^t = DM\theta, \quad -\mathbf{l}_{lim} \le \mathbf{p}_\ell^t \le \mathbf{l}_{lim}, \quad t \in \mathscr{T}, \tag{7}$$

where the components of the vector θ are the voltage angles at each node, B is the reduced susceptance matrix and B^{-1} is its inverse, the variable $\mathbf{p}_k$ is the nodal power injection vector, the variable $\mathbf{p}_\ell^t$ is the vector of power flow on each line, the elements of the diagonal matrix D are the negative susceptance of each line, M is the nodal-branch incidence matrix, and the vector $\mathbf{l}_{lim}$ is the power limit of each line of the network. More details of the direct current (DC) power flow formulation presented above are found in (Seifi and Sepasian 2011). The DC power balance of the system is defined as follows:

$$\sum_{i\in\mathscr{I}_k} P_i^t + \sum_{l\in\mathscr{L}_{k,in}} P_{\ell l}^t = L_k^t + \sum_{l\in\mathscr{L}_{k,out}} P_{\ell l}^t, t \in \mathscr{T}, k \in \mathscr{K}, \tag{8}$$

where $\mathscr{I}_k$ represent the set of generating units located at bus k, $\mathscr{L}_{k,in}$ is the subset of lines injecting power to node k, and $\mathscr{L}_{k,out}$ is the subset of lines taking power generated at node k. The dual variables associated to (8) are called locational marginal prices (LMP) or nodal prices.

The system reserve is defined with the 3% rule proposed in (Piwko, Clark, Freeman, Gordan, and Miller 2010), which states that the total reserve of the system should be at least 3% of the total forecasted demand at each period of time. Let $R_{tot}^t = 0.03\sum_{k\in\mathscr{K}} L_k^t$ then the system reserve constraint is formulated as:

$$R_{tot}^t \le \sum_{i\in\mathscr{I}} R_i^t, t \in \mathscr{T}. \tag{9}$$

The operational rules of the units include generation limits, start-up of the units, ramping constraints, generation reserve levels, and minimum up and down scheduling time. The mathematical formulation of these constraints are listed below:

$$P_i^- w_i^t \le P_i^t \le P_i^+ w_i^t, \quad z_i^t = w_i^t - w_i^{t-1}, \quad \underline{R}_i \le P_i^t - P_i^{t+1} \le \overline{R}_i, \quad i \in \mathscr{I}, t \in \mathscr{T}, \tag{10}$$

$$(P_i^t + R_i^t) - (P_i^{t-1} - R_i^{t-1}) \le \overline{R}_i, \quad \underline{R}_i \le (P_i^t - R_i^t) - (P_i^{t-1} + R_i^{t-1}), \quad i \in \mathscr{I}, t \in \mathscr{T}, \tag{11}$$

$$\textstyle\sum_{\tau\in\mathscr{U}_{i,t}} z_i^\tau \le w_i^{t-1}, \quad \mathscr{U}_{i,t} = \{t - UT_i + 1,\dots,t| \text{ if } UT_i \le t\}, \quad i \in \mathscr{I}, t \in \mathscr{T}, \tag{12}$$

$$\textstyle\sum_{\tau\in\mathscr{D}_{i,t}} z_i^\tau \le 1 - w_i^{t-1} \quad \mathscr{D}_{i,t} = \{t+1,\dots,t+DT_i| \text{ if } |T - DT_i| \le t\}, \quad i \in \mathscr{I}, t \in \mathscr{T}, \tag{13}$$

where P_i^- and P_i^+ are the generation limits, $\underline{R}_i$ and $\overline{R}_i$ are the ramping limits, and the parameters UT_i and DT_i represent the minimum up and down scheduling time for each unit $i \in \mathscr{I}$. The UC model is formulated as the following mixed-integer optimization problem:

$$\min_{\mathbf{w},\mathbf{z},\mathbf{p},\mathbf{r},\mathbf{p}_\zeta,\mathbf{p}_\ell} F(\mathbf{w},\mathbf{z},\mathbf{p}) \tag{14}$$

$$\text{subject to:} (7),(8),(9),(10),(11),(12),(13). \tag{15}$$

2.3 Microgrid Location and Power Transaction Pricing

For a vector $x \in \mathbb{R}^T$ its euclidean norm is denoted as $\|x\| := \sqrt{\sum_{t\in\mathscr{T}}(x^t)^2}$. Let μ_k^t be the optimal dual variable associated to constraint (8) for node $k \in \mathscr{K}$ at time $t \in \mathscr{T}$ with a forecasted load level L_k^t, and represent the nodal price as $\mu_k := [\mu_k^1, \ldots, \mu_k^T], k \in \mathscr{K}$.

In this study, congestion of nodes is measured with the euclidean norm of the nodal prices. The sorting $\|\mu_{k_1}\| \leq \cdots \leq \|\mu_{k_K}\|$ provides a partial order for nodal intensity-congestion from uncongested to congested, which is denoted as $k_1 \preceq \cdots \preceq k_K$. This partial order is used to strategically locate the microgrid in the network.

In order to find appropriate import/export price strategies that are beneficial for both the microgrid and the power system, a congestion study of the power system is conducted. After selection of a candidate location for the microgrid, k^*, a sensitivity analysis on the nodal price μ_{k^*} is performed by solving the UC model for different nodal load levels $\mathbf{l}_{k^*}$. The main goal of this analysis is to obtain an accurate understanding of congestion behavior at k^*; the nodal prices generated are used to incorporate congestion information into the functions $\kappa_i^t(\cdot), \kappa_e^t(\cdot)$.

Section 3 provides a validation, via simulation, of the price strategy described above as well as behavior of the microgrid located at nodes with different intensity-congestion levels.

3 NUMERICAL RESULTS

In this section, the model described in Section 2 is applied to the IEEE 30-bus test system, shown in Figure 1. In this context, the model is used to explore the impact of import/export pricing strategies on transmission congestion conditions in the main grid. A line diagram of the 30-bus network is given in Figure 1, showing the location of loads and generation. The interested reader is referred to (Zimmerman, Murillo-Sanchez, and Thomas 2009, case30) for detailed parameters of the system.

The objective of this work is to illustrate the potential for a microgrid to attenuate congestion on the main transmission network. To this end, the problem is considered from two perspectives; in Section 3.1, the placement of the microgrid on the network is explored, followed by Section 3.2 which compares import/export pricing strategies, for the purposes of motivating the microgrid to behave in a way that is beneficial to the main network.

The overall approach of this study is the interconnection of the microgrid energy management model, described in Section 2.1, with the transmission level unit commitment and dispatch model, described in Section 2.2. The procedure for integrating these models is as described in Algorithm 1.

3.1 Microgrid Location

The microgrid has three diesel generators with an aggregate capacity of 4.95MW. The generation cost is 3$/MW for each generator. There is one energy storage unit with an initial state of charge (SoC) of 5MWH and total capacity 10MWH. The charging/discharging limit is 3MW, and the cost of storing energy is 0.1$/MWH. The aggregated time varying non-dispatchable load ranges from 3.4MW to 4.1MW. The aggregated dispatchable load ranges from 2MW to 3.6MW with an incentive reward of 3.03$/MW. The aggregated photovoltaic (PV) generator has a limit of 10MW. Loads and renewable generation are selected to represent summer conditions from the NREL Western Wind and Solar Integration Study (GE Energy 2010). This configuration allows the microgrid to be managed to maximize use of renewable resources

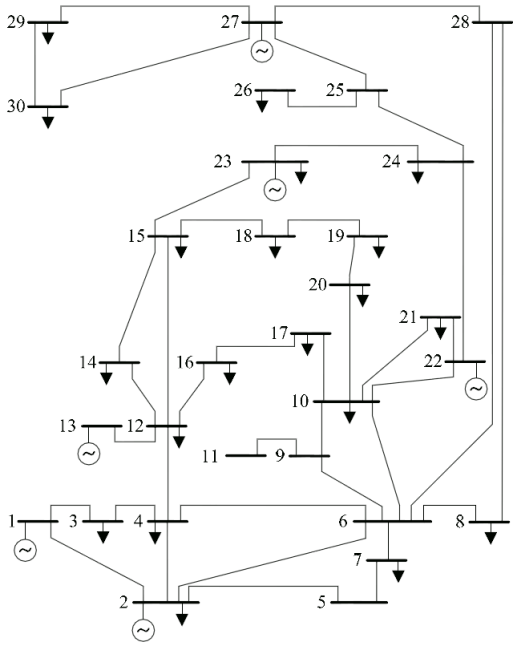

Figure 1: IEEE 30 Bus Network Diagram.

through storage and flexible loads, though the import (purchase) of additional power and export (sale) of excess generation to the main grid, is possible.

To illustrate a baseline, the first case considered is of an uncongested transmission system, followed by the case of a congested network, with and without the microgrid. In the initial comparisons of this section, the uncertain generation of the PV generator are represented by the expected daily trajectory of July 2006 from (GE Energy 2010).

Algorithm 1 Simulation Approach

1: Determine candidate node k^*, for microgrid as described in Section 2.3.
2: Solve unit commitment and dispatch of transmission system (without microgrid) for range of loads at k^*, as described in Section 2.2, to determine the nodal price of power at node k^*, for each load level.
3: For $t \in \mathscr{T}$, construct piecewise linear (PWL) import cost function $\kappa_i^t(\cdot)$ (withdrawal at node k^*), using the LMP from step 2 as the slope of the linear pieces.
4: For $t \in \mathscr{T}$, construct PWL export cost function $\kappa_e^t(\cdot)$ (injection at node k^*), where the slope of the linear pieces is equal to $0.8\times$ nodal price found in step 2.
5: Given the PWL functions $\kappa_i^t(\cdot), \kappa_e^t(\cdot)$, allow microgrid to optimize procurement strategy for given $\mathbf{p}_v$, $\mathbf{p}_g$, $\mathbf{b}$, $\mathbf{p}_d$, as described in Section 2.1.
6: Re-solve transmission-level unit commitment, given injection/withdrawal schedule determined in step 5, to determine congestion status.

3.1.1 Uncongested Main Grid

In the uncongested case, the line flows are closest to the line limit between buses six and eight. In the congested case in the next section, the LMPs at bus eight are the highest. Thus the LMPs at bus eight are used as a proxy to compare the condition of the main grid with and without the microgrid in Table 1.

Table 1: Comparison of LMPs at bus 8 of the main network, with and without connected microgrid.

Case \ t	1	2	3	4	5	6	7	8	9	10	11	12	13	14	15	16	17	18	19	20	21	22	23	24
LMP without MG	3.88	3.83	3.82	3.81	3.82	3.82	3.85	3.93	3.97	3.99	4.02	4.01	4.03	4.04	4.03	4.04	4.03	4.00	3.98	3.96	3.95	3.94	3.93	3.91
LMP with MG	3.88	3.84	3.83	3.81	3.83	3.82	3.85	3.93	3.96	3.97	3.99	3.98	4.00	4.01	4.03	4.04	4.03	4.00	3.98	3.96	3.95	3.94	3.93	3.92

The comparison in Table 1 shows that when the main network is free of congestion, the inclusion of the microgrid at bus eight has very little impact on the main grid. This is due to the relatively small contribution of the microgrid compared to the size of the main network, in conjunction with the available transmission capacity in an uncongested state.

3.1.2 Congested Main Network

Alternatively, the situation is considered wherein congestion exists between buses six and eight. This congestion is induced by increasing the size of the load on bus eight until the line reaches its flow limit. A first consideration is the impact of the microgrid location on congestion within the network. For brevity, we give results of the congestion and LMP changes at three typical locations for placing the microgrid including the lowest LMP bus (bus 6), highest LMP bus (bus 8) and a bus with an intermediate LMP (bus 17). The results are shown in Table 2.

Table 2: Comparison of location effect of microgrid using LMPs at bus 8 of the main network, red font indicates congestion.

Case \ t	1	2	3	4	5	6	7	8	9	10	11	12	13	14	15	16	17	18	19	20	21	22	23	24
No MG	3.91	3.87	3.86	3.84	3.85	3.85	3.88	3.96	4.04	4.41	5.80	5.40	6.26	6.86	6.56	7.01	6.16	4.69	4.20	3.99	3.98	3.97	3.96	3.94
MG @ bus 6	3.91	3.87	3.86	3.84	3.85	3.85	3.88	3.96	4.07	4.56	6.10	5.75	6.59	7.16	6.63	7.01	6.16	4.69	4.20	3.99	3.98	3.97	3.96	3.95
MG @ bus 17	3.91	3.87	3.86	3.84	3.85	3.85	3.88	3.96	4.05	4.46	5.93	5.54	6.39	6.98	6.59	7.01	6.16	4.69	4.20	3.99	3.98	3.97	3.96	3.95
MG @ bus 8	3.91	3.87	3.86	3.84	3.85	3.85	3.88	3.96	4.00	4.01	4.03	4.01	4.03	4.05	4.05	4.06	4.29	4.02	4.02	3.99	4.00	4.08	3.96	3.95

Note that values in red font indicate congestion in the line between buses six and eight during the periods highlighted. Examination of Table 2 shows that in the congested base case, without the microgrid, the line is congested during hours 11 through 17. The results also show that placement of the microgrid at bus six (lowest LMP) has the effect of increasing the LMPs at bus eight during the congested hours, indicating that this placement is exacerbating the base-case congestion. Conversely, placement of the microgrid at bus eight, where LMPs are highest, has the opposite impact; effectively eliminating the high LMPs that are symptomatic of congestion in the system.

This effect results from the economic incentive for the microgrid to restrain its import (withdrawal) during congested periods, and instead to encourage higher export to the main network, through use of its renewable resources and storage capabilities. The comparisons of this section are based on the use of mean daily PV generation levels in the microgrid. In order to observe the congestion impacts within the transmission grid, it is also useful to consider uncertainty in more detail, which is the focus of Section 3.2.

3.2 Pricing Scheme Simulations

In this section the interaction between the microgrid, the transmission system, and grid congestion conditions are considered under uncertain solar resource availability. Specifically, in this case the model is used to simulate various import/export pricing schemes for the microgrid. These simulations use 31 daily PV

generation scenarios from the WWSIS synthetic data set (GE Energy 2010) for July 2006, shown in Figure 2.

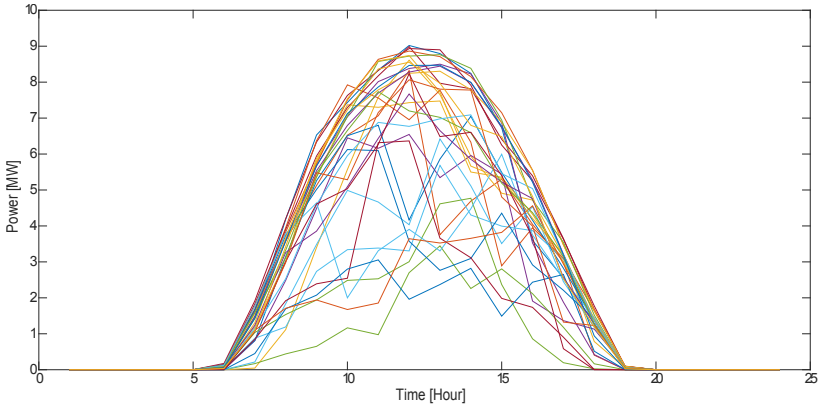

Figure 2: Solar Generation Scenarios.

The piecewise linear cost functions for the microgrid, under congested and uncongested conditions, respectively, are give in Figure 3 and 4.

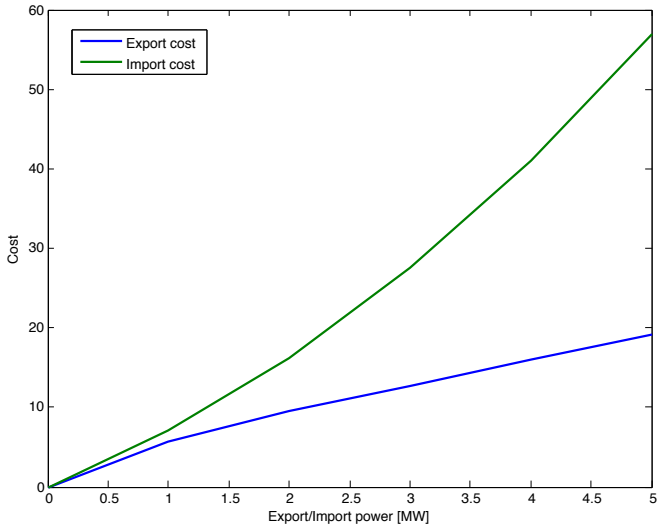

Figure 3: PWL import/export cost functions $\kappa_i^{17}(p), \kappa_e^{17}(p)$: Congested case.

It is worth noting that the import cost is a convex function, and is always higher than the concave function of the export cost, guaranteeing convexity of the objective function (5). The structure of the PWL functions $\kappa_e^t(\cdot), \kappa_i^t(\cdot), t \in \mathscr{T}$ are such that actions which increase congestion are penalized proportionally. Specifically, in the congested case, the slope of the import cost increases with larger withdrawals, meaning it is increasingly more costly to import. Conversely, the slope of the export decreases with larger injections, to reflect the decreasing marginal benefit of these injections on congestion. Finally, the cost function for import (export) to (from) the microgrid is highly linear in the uncongested case, given that the transmission system is relatively unaffected by imports/exports on the scale of the microgrid, due to the excess capacity.

The first result of this analysis are given as empirical distributions for usage level of the congested line in the main network, using three pricing schemes: 1) PWL case which uses the piecewise linear cost function previously described in this section; 2) FLMP case uses $\kappa_i^t(p) = \mu^t, \kappa_e^t(p) = 0.8\mu^t$ where μ is the vector whose components are the initial LMP network solution (first row of Table 2); 3) HLMP case

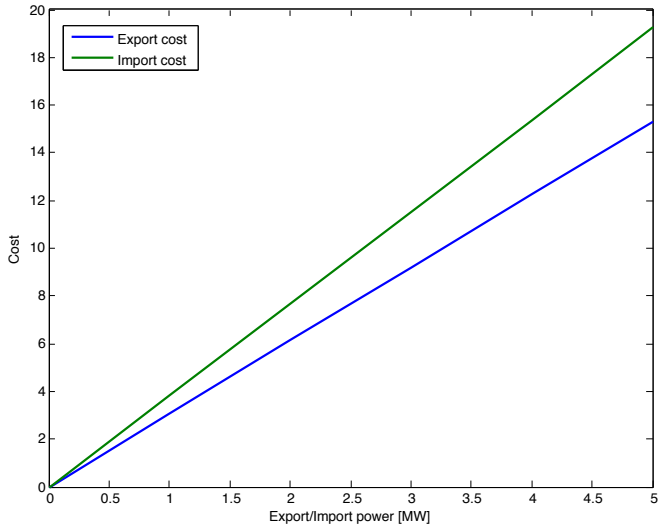

Figure 4: PWL import/export cost functions $\kappa_i^4(p), \kappa_e^4(p)$: Uncongested case.

uses $\kappa_i^t(p) = \beta, \kappa_e^t(p) = 0.8\beta$ where $\beta = \max_{t \in \mathcal{T}}\{\mu^t\}$. Figures 5, 6 and 7 illustrate line usage for each of these three cases.

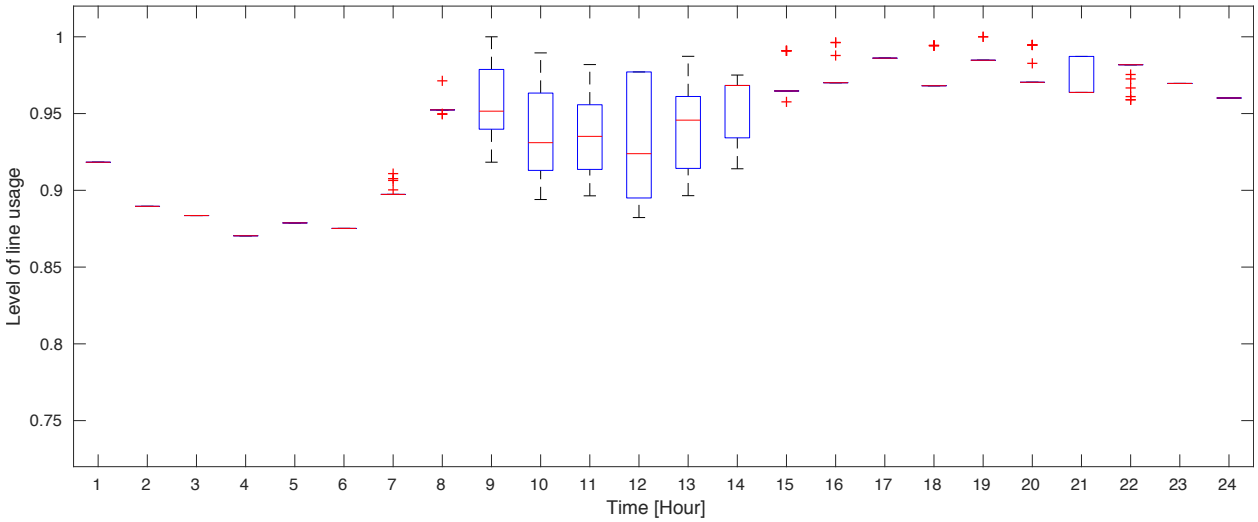

Figure 5: Usage level of the line from bus 6 to bus 8 for PWL.

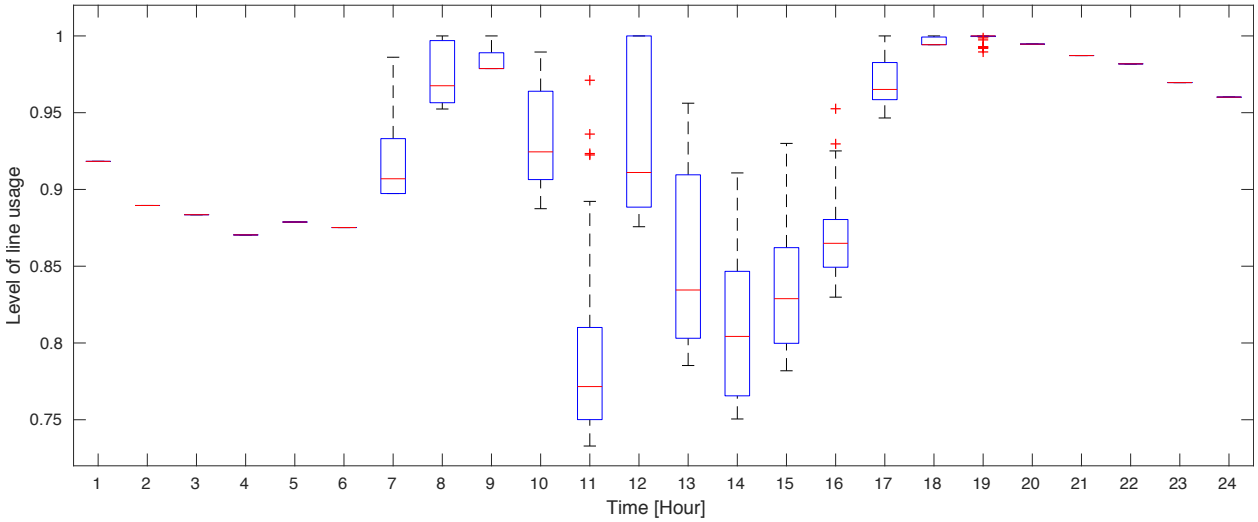

Figure 6: Usage level of the line from bus 6 to bus 8 for FLMP.

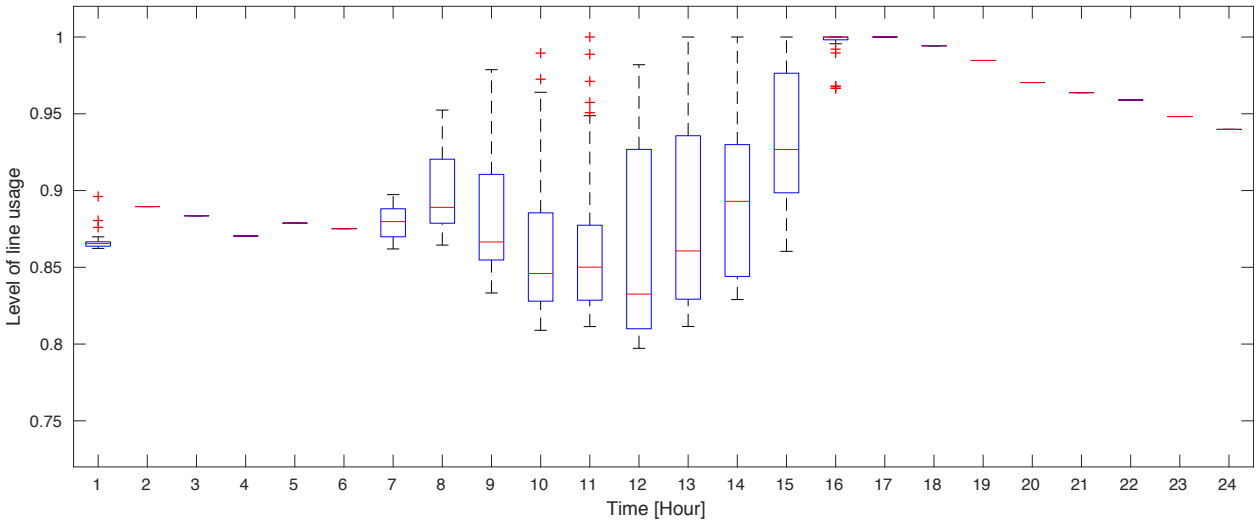

Figure 7: Usage level of the line from bus 6 to bus 8 for HLMP.

Examination of Figures 6 and 7 show that the HLMP and FLMP cases show significantly more variance in line use, than the PWL pricing scheme. To summarize the influence of these pricing schemes on congestion conditions, the incidences of congestion are summarized in Table 3.

Table 3: Frequency of congestion incidents occurring on the branch connecting buses 6 and 8.

t	1	2	3	4	5	6	7	8	9	10	11	12	13	14	15	16	17	18	19	20	21	22	23	24
PWL	0	0	0	0	0	0	0	0	1	0	0	0	0	0	0	0	0	0	2	0	0	0	0	0
FLMP	0	0	0	0	0	0	0	8	6	0	0	9	0	0	0	0	6	8	22	0	0	0	0	0
HLMP	0	0	0	0	0	0	0	0	0	0	1	0	4	4	4	23	31	0	0	0	0	0	0	0

As shown in Table 3, the piecewise linear pricing scheme results in very few incidents of transmission congestion in hours 9 and 19. In contrast, the FLMP pricing scheme results in nearly 60 incidents of congestion spread over six hours of the day and the higher fixed pricing scheme (HLMP) leads to transmission

level congestion nearly 75 times over seven hours of the day. These results clearly illustrate that the use of a responsive pricing scheme, such as the PWL scheme proposed here, has a positive effect on microgrid interactions with the transmission system.

4 CONCLUSIONS

In this work, an empirical study is undertaken to explore interaction between the transmission system and a microgrid. Of primary interest is the effect of this interplay on the congestion conditions in the main network. This analysis uses a coupled model between the unit commitment and dispatch of the transmission system, and the energy management solution for the microgrid. A case study of the IEEE 30-bus system is implemented to explore this approach.

The results of this work show that, in a congested system, the most effective location for the microgrid is the load-bus with the highest nodal price for power. The effect of this placement shows positive outcomes for the transmission system, through elimination of the existing congestion. Placement at locations with lower nodal prices has no effect on congestion in the best case, and exacerbates congestion problems in the worst case of placement at the source node of a congested line.

Given the placement of a microgrid in a congested network, pricing strategies are important to induce the microgrid to behave in a manner that attenuates congestion in the transmission system, while optimizing energy management within the microgrid. The results in Section 3.2 show that fixed prices for power injections/withdrawals from the transmission system send ineffective signals to the microgrid, regardless of the level of those prices. Conversely, the piecewise linear cost function, obtained from sensitivity analysis within the transmission system, is highly effective in ensuring that microgrid develops a strategy that is effective for both its consumers and the transmission system as a whole.

ACKNOWLEDGMENTS

This work was partially supported by the National Science Foundation under grant no. ECCS-1453615.

REFERENCES

Afkousi-Paqaleh, M., A. Abbaspour-Tehrani-fard, M. Rashidinejad, and K. Y. Lee. 2010. "Optimal Placement And Sizing Of Distributed Resources For Congestion Management Considering Cost/Benefit Analysis". *Power and Energy Society General Meeting*.

Afkousi-Paqaleh, M., A. R. Noory, A. A. T. F., and M. Rashidinejad. 2010. "Transmission Congestion Management Using Distributed Generation Considering Load Uncertainty". *Power and Energy Engineering Conference (APPEEC)*:1–4.

Bertsekas, D. 1999. *Nonlinear Programming*. second ed. Athena Scientific.

Chun-Hao, L., and A. Nirwan. 2012. "Alleviating Solar Energy Congestion In The Distribution Grid Via Smart Metering Communications". *Institute of Electrical and Electronics Engineers Transactions on Parallel and Distributed Systems*.

EPA 2016. "Draft Inventory Of U.S. Greenhouse Gas Emissions And Sinks: 1990-2014". Technical report, United States Environmental Protection Agency. https://www3.epa.gov/climatechange/ghgemissions/usinventoryreport.html.

GE Energy 2010. "Western Wind And Solar Integration Study". Technical Report AAM-8-77557-01, National Renewable Energy Laboratory. http://www.nrel.gov/docs/fy10osti/47434.pdf.

Kumar, N., P. Dutta, and L. Xie. 2011. "Optimal DG Placement For Congestion Mitigation And Social Welfare Maximization". In *North American Power Symposium (NAPS), 2011*, 1–5.

Labrini, H., A. Gad, R. A. ElShatshat, and M. M. A. Salama. 2015. "Dynamic Graph Based Dg Allocation For Congestion Mitigation In Radial Distribution Networks". In *Power Energy Society General Meeting*, 1–5. Institute of Electrical and Electronics Engineers.

Liu, J., M. G. Martinez, B. Li, J. Mathieu, and C. L. Anderson. 2016. "A Comparison Of Robust And Probabilistic Reliability For Systems With Renewables And Responsive Demand". In *49th Hawaii International Conference on System Sciences (HICSS)*, 2373–2380.

Liu, J., M. M. A. Salama, and R. R. Mansour. 2005. "Identify The Impact Of Distributed Resources On Congestion Management". *Institute of Electrical and Electronics Engineers Transactions On Power Delivery* 20 (3): 1998–2005.

Martinez, G., N. Gatsis, and G. Giannakis. 2013. "Stochastic Programming For Energy Planning In Microgrids With Renewables". In *5th International Workshop on Computational Advances in Multi-Sensor Adaptive Processing (CAMSAP), 2013*, 472–475. Institute of Electrical and Electronics Engineers.

Martinez, G., Y. Zhang, and G. Giannakis. 2014. "An Efficient Primal-Dual Approach To Chance-Constrained Economic Dispatch". In *North American Power Symposium (NAPS), 2014*, 1–6.

Mohsenian-Rad, H. 2015. "Coordinated Price-Maker Operation Of Large Energy Storage Units In Nodal Energy Markets". *Institute of Electrical and Electronics Engineers Transactions on Power Systems* 31 (1): 1–12.

Nabavi, S. M. H., S. Hajforoosh, and M. A. S. Masoum. 2011. "Placement And Sizing Of Distributed Generation Units For Congestion Management And Improvement Of Voltage Profile Using Particle Swarm Optimization". In *Innovative Smart Grid Technologies Asia (ISGT), 2011*, 1–6. Institute of Electrical and Electronics Engineers.

Nayanatara, C., J. Baskaran, and D. P. Kothari. 2015. "Simulated Annealing Approach For Congestion Minimization Using Distributed Power Generation". *Computation of Power, Energy Information and Commuincation (ICCPEIC)*:276–281.

Piwko, R., K. Clark, L. Freeman, G. Gordan, and N. Miller. 2010. "Western Wind And Solar Integration Study". Technical report, National Renewable Energy Laboratory.

Seifi, H., and M. S. Sepasian. 2011. *Electric Power System Planning: Issues, Algorithms And Solutions*. Springer Berlin Heidelberg.

Tahanan, M., W. van Ackooij, A. Frangioni, and F. Lacalandra. 2015. "Large-scale Unit Commitment Under Uncertainty". *4OR* 13 (2): 115–171.

Wu, L., and M. Shahidehpour. 2010. "Accelerating The Benders Decomposition For Network-Constrained Unit Commitment Problems". *Energy Systems* 1 (3): 339–376.

Zhang, Y., N. Gatsis, and G. Giannakis. 2013. "Robust Energy Management For Microgrids With High-Penetration Renewables". *Institute of Electrical and Electronics Engineers Transactions on Sustainable Energy* 4 (4): 944–953.

Zimmerman, R., C. Murillo-Sanchez, and R. Thomas. 2009. "MATPOWER's Extensible Optimal Power Flow Architecture". In *Power Energy Society General Meeting, 2009. PES '09*, 1–7.

AUTHOR BIOGRAPHIES

JIALIN LIU is a Ph.D. Candidate in the Department of Electrical and Computer Engineering at Cornell University. His current research focus is the optimization of electric power grid operation with significant penetration of renewable energy. His email address is jl3455@cornell.edu.

M. GABRIELA MARTINEZ is a Research Associate in Health Systems Engineering at the Mayo Clinic Kern Center for Science of Health Care Delivery. Her primary interests are stochastic optimization, numerical analysis, simulation and their applications. Her email address is martinez.maria@mayo.edu.

C. LINDSAY ANDERSON is an Assistant Professor in the Department of Biological and Environmental Engineering at Cornell University. Her research interests focus on the application of systems modeling and optimization to energy and the environment. Her email address is cla28@cornell.edu.